Int J Adv Manuf Technol (2018) 94:1429–1439
DOI 10.1007/s00170-017-1015-5

ORIGINAL ARTICLE

Active control of high-frequency tool-workpiece vibration in micro-grinding

Xiaohui Jiang[1] · **Miaoxian Guo**[1] · **Beizhi Li**[2]

Received: 16 June 2017 / Accepted: 17 August 2017 / Published online: 29 August 2017

Abstract The high-frequency tool-workpiece vibration in micro-grinding plays a pivotal role in influencing surface generation in micro-grinding. To overcome the problems coming with the process vibration, this paper presents the implementation and testing of an active vibration control platform that can be used to suppress the high-frequency relative vibrations between the tool and the workpiece during the micro-grinding processes. The platform with small actuator displacement and high-resonance frequency is applied as workpiece holding platform and can cancel vibration in real time by sensing the tool vibration with the vibrometer. The active control system developed here is based on an adaptive filtering algorithm; the tool vibrations and relative vibrations in micro-grinding process are treated as system disturbances and control target respectively. Cutting experiments are performed to demonstrate the vibration reduction and to validate the effectiveness of the control system; the results show that the developed system works well in micro-grinding vibration cancelation.

Keywords Active control · Tool-workpiece · Vibration · Micro-grinding · Workpiece holding platform

✉ Miaoxian Guo
miaoxian.guo@live.com

[1] College of Mechanical Engineering, University of Shanghai for Science and Technology, No.516 Jungong Road, Shanghai 200093, China

[2] College of Mechanical Engineering, Donghua University, No.2999 North Renmin Road, Shanghai 201620, China

1 Introduction

Highly accurate miniaturized components are increasingly in demand for various industries such as aerospace, electronics, automotive, and so on. Micro-machining is an ultra-precision material removal process to achieve micro-accuracy and nanometer finish [1]. In micro-machining filed, the micro-grinding is an approach opens the option to structure hard and brittle materials which are particularly wear resistant for molding applications and durable against chemicals for fluid reactors [2]. However, machining vibration is an intrinsic physical phenomenon, which would easily influence the surface roughness and subsurface damage in micro-grinding. And in extreme situations, it may lead to chatter and destabilize the cutting system.

Due to the negative influence of grinding vibration upon surface roughness and subsurface damage, researchers have experimentally and theoretically studied the topic. Hassui and Diniz studied the relation between the process vibration signals and workpiece quality (including mean roughness, circularity, and burning) on plunger cylindrical grinding of steel [3]. Taking the relative vibration between grinding wheel and workpiece into account, alongside the abrasive grain trajectory equation, Cao et al. established a new analysis and simulation model for surface topography of the grinding process is established [4]. Chen et al. proposed a new model to analyze the relationship between surface roughness on the basis of grinding kinematics analysis and indentation fracture mechanics of brittle materials taking the wheel spindle vibration into account [5]. Furthermore, Chen et al. studied the primary factors affecting surface quality and developed a theoretical model for surface generation in grinding silicon carbide (SiC), considering the geometrical kinematics and tool micro-vibration in the grinding operation [6]. Wang et al. proposed an efficient new method for simulating the surfaces of

grinding wheel and grinding workpieces, the model started from generating the topography of wheel surface, and the abrasive grain trajectory equations were established according to grinding kinematics [7]. As in the micro-grinding area, few work focus on the process vibration's influence on surface and subsurface quality, even though the process vibration should be taken more seriously.

To overcome the problems coming with the process vibration, researchers have made considerable efforts to control and attenuate the vibrations during cutting process. There are many types of vibration control methods in machining filed. One of the traditional passive vibration control methods is the machining parameter optimization for vibration attenuating purpose. However, According the previous research of Grigoriev et al. machining parameter optimization is not only simply related to vibration, it would also influence the machining mechanism, efficiency, etc [8–10]. In another passive method, Duncan et al. introduced the dynamic absorbers to reduce the cutting vibration [11], Muhammad et al. give a review of dynamic damping of machining vibration [12], and all the researches indicate that the effectiveness is frequency limited and directly related with the dynamic characteristics of the machining system.

Apart from the passive vibration control method, increasing attentions have been paid to the active control on cutting vibration. One way to active control the cutting vibration in process is the active damping of machine tool: the control system is designed to add damping at the natural frequencies of control objects so that the damped modes are sufficiently stabilized. For this control type, Ganguli et al. demonstrate the effect of active damping on regenerative chatter instability for a turning operation [13]; Tewani et al. used a piezoelectric actuator as an active dynamic absorber to suppress chatter in the boring process [14]. Furthermore, Zhang et al. applied the active damping to avoid the chatter avoidance in machining process [15]. Chen and Liu presented a novel multifunctional magnetic actuator, which not only damps the vibration of machine tools but also measures the cutting force in real time [16].

Another active control method is the vibration direct control system that cancels vibration in real time by sensing cutting vibrations, then expanding and contracting actuators along the opposite direction to filter out the motion. In general, the active control system is for tool-spindle unit or workpiece. Ei-Sinawi et al. developed optimal vibration control systems for turning operations by using active tool holder [17]. Zaharnah et al. further developed optimal vibration control systems in both feed and radial directions to suppress the vibrations in cutting [18]. Zhang et al. also use active magnetic bearing or piezo actuators to control spindle vibrations [19]. However, it is difficult to run a sophisticated vibration control system for a rotating tool or spindle. Therefore, Rashid and Nicolescu developed an active control system for palletized workholding system in milling operations and validated the vibration reduction performance [20]. Brecher et al. proposed the active workpiece holder with two high-dynamic axes controlled by piezoelectric actuators onto a milling machine. With these additional highly dynamic axes near the tool center point, the active workpiece holder offers possibilities to prevent chatter vibrations [21]. Long et al. developed an active milling vibration control system to suppress the relative vibrations between the tool and the workpiece during the milling processes and improved the rough of surface finish significantly [22].

In previous researches, whatever the vibration's influence on surface and subsurface quality, the vibration process is confined to tradition cutting process, and the frequency components of cutting vibrations to be controlled effectively are limited. While the vibration control in micro-grinding is not well studied, in which the control accuracy and control frequency are much higher. The vibration in micro-grinding is mainly induced by the tool and spindle system, which is the periodic variation of the relative displacement between tool and workpiece. The relative vibration between tool and workpieces inevitably encountered to deteriorate surface quality and surface profiles at the microscopic level.

In this work, an active vibration control system with small actuator displacement and high-resonance frequency is presented, to attenuate the relative vibrations between the wheel and workpiece. The two degree of freedoms (DOFs) active workpiece holding platform is tested through static and dynamic approach. Then, the control system modeling and controller design are proposed to meet the requirement of micro-grinding process. At last, an engineering experiment is conducted to verify the effective of the active control system.

2 Micro-grinding active vibration platform design

2.1 System design

The workpiece holding platform is developed to control the relative vibration between the tool and the workpiece. As showed in Fig. 1, it cancels vibration in real time by sensing vibration, then expanding and contracting piezoelectric actuators to filter out the motion. The platform has independent movement of two directions and can be simplified as two independent controlled objects. The platform is fixed on the machine table, so the connection between the machine and the platform is regarded approximate rigid connection, then the workpiece and the moving part of the platform have a total mass of m, the system consists of a spring K, and a damping C in parallel with a force actuator F_c; x_w stands for the displacement of workpiece motion, and x_t stands for the displacement of the tool vibration. The objective of the control system is to cancel the relative vibration of x_t-x_w. For the force actuator applied to the workpiece, the governing equations are as follows:

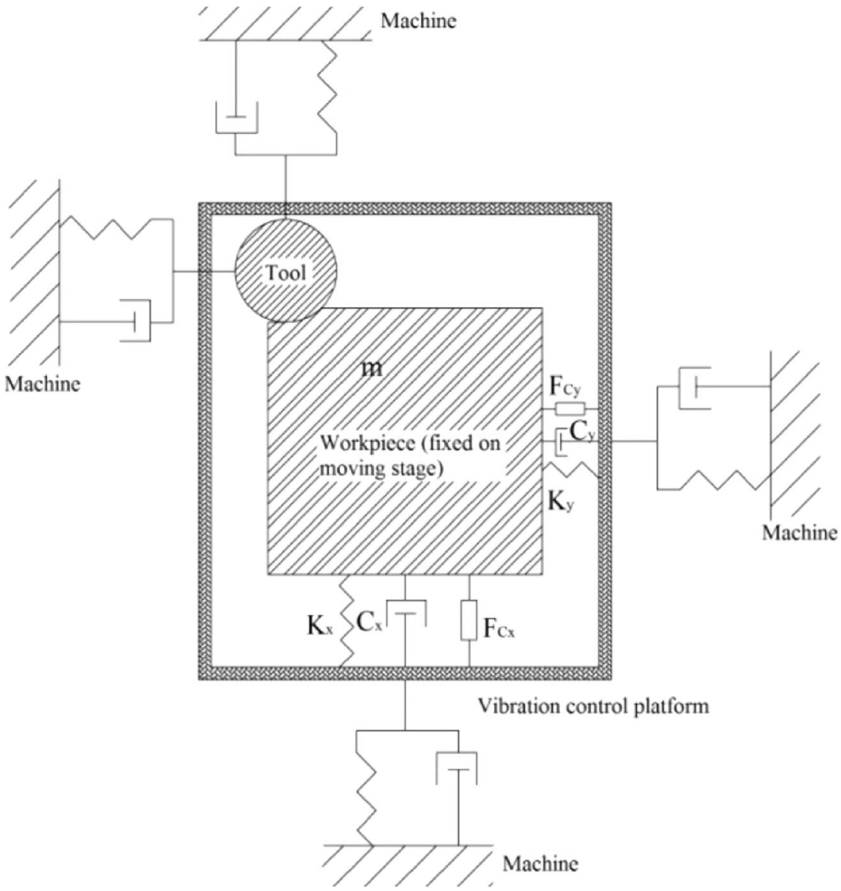

Fig. 1 System dynamics of the active control platform in micro-grinding

$$m\ddot{x}_w + C\dot{x}_w + Kx_w = F_c \tag{1}$$

2.2 Control parameter design

Similar to milling, the micro-grinding process involves both self-excited and forced vibration. In the previous study, it is found the dynamic micro-grinding force due to intermittent cutting loads on the workpieces is usually less than 1 N, and the tool dynamic response displacement is 0.1–0.6 μm, which always occurs at a frequency of spindle rotating speed [23]. Also, according to the rotary accuracy calibration and test results, the spindle produced a 0–1.5-μm vibration without load. Therefore, in a stable micro-grinding process, they are the dominant vibrations and both occur at rotating frequency. In order to control the process vibration between tool and workpiece, the control system focused on the radial displacement of the main vibration frequency.

In our study, the micro-grinding machine with the Fischer AG spindle has a maximum speed of 120,000 rpm, and the operations are typically in the range of 60,000–90,000 rpm. Since for rotating speed of R, the vibration frequency is

$$f = R/60 \tag{2}$$

The main control frequency range is 1000–1500 Hz, which is much higher than the traditional machining. Since control systems are based on the performance of the vibration sensor, the characteristics of the piezoelectric ceramic actuator system, the hardware and software of the controller, and the upper vibration frequency limit is set at about 1500 Hz. To avoid the resonance vibration of active workpiece holding platform, the first-order resonance frequency of the platform should be more than 1.4 times the main frequency, namely more than 2100 Hz.

In the workpiece holding platform, the piezoelectric actuators with a fast response, high stiffness, high resolution, and long period life are applied as driving units for the platform. And flexure hinges are implemented in platform structure to transform force and displacement generated by actuator to workpiece holder in the two directions dependently. Since the flexure hinge in the system is based on the elastic deformation of solid material, the system can provide smooth and continuous motion. As developed in Long's research [22], in a typical notched hinge, the bending stiffness of the hinge K_h is given as

$$K_h = \frac{2E \times h \times t^{\frac{5}{2}}}{9\pi \times R^{\frac{1}{2}}} \tag{3}$$

Where, R is the notch radius, t is the thickness, h is the width of the hinge, and E is the Young's modulus of the flexure material, respectively. The platform should be designed with two orthogonal DOFs along X- and Y-directions. The static stiffness of the platform should be of this form:

$$K_{x/y} = \frac{4E \cdot h \cdot t^{\frac{5}{2}}}{9\pi \cdot L_{x/y}^2 R^{\frac{1}{2}}} \tag{4}$$

Where the subscripts x and y refer to the X- and Y-directions and L_x and L_y are the distances between the axis of actuators and the notched hinges, respectively. In the paper, the platform has the maximum push force of 1000 N and maximum pull force of 200 N in both X- and Y-direction, and the travel distances of the platform should more than 10 μm (at driving voltage of 120 V) along X- and Y-directions.

In process situation, active vibration cancelation should be used to control the dynamic behavior, the voltage and frequency can affect the capacitor voltage, and the relation can be expressed as

$$U = I/2\pi fC \tag{5}$$

Therefore, the dynamic travel distance at working frequency should cover the maximum main vibration amplitude of self-excited and forced vibration (1.5 and 0.6 μm).

3 Active workpiece holding platform performance testing and analysis

The dynamic travel distance of the workpiece holding area and the first-order resonance frequency are two key performance parameters. The dynamic travel distance determines the level of vibration amplitude can be canceled, and the resonance frequency is the ability that the platform can be applied dynamically to avoid the resonance of exciting force. To verify the performance of the manufactured platform as shown in Fig. 2, the frequency response function (FRF) test and displacement output experiment is conducted on it.

In the test, the vibration displacement and travel distance are obtained by a KEYENCE® laser displacement sensor LK-H020 and controller LK-HD500. The signals of forces are collected in the impact experiments by a PCB® hammer 086C02, and the signals of forces and vibration are recorded and analyzed with LMS® SCADAS mobile [24].

3.1 FRF test by impact test

To identify the dynamic properties of the system, a modal analysis was carried out using impact hammer testing. The frequency response functions are collected and studied in the impact experiments as indicated in Fig. 3. Further analysis can be obtained, the first-order resonance frequencies of X-direction and Y-direction were 2499 and 2407 Hz, respectively, this analysis indicated the expected performance region of the active control system. In micro-grinding, most of the exciting energy that was concentrated at frequency of the spindle speed in this case did not coincide with any of the system's natural frequencies.

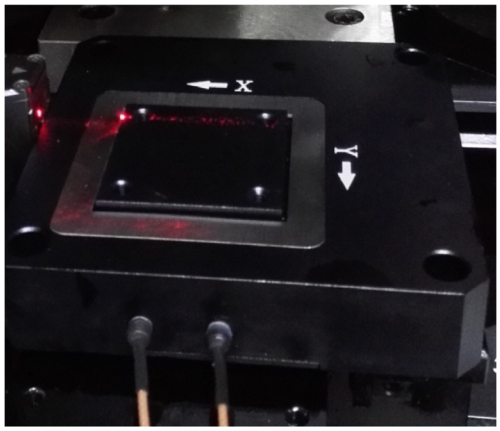

Fig. 2 Active workpiece holding platform

3.2 Static and dynamic travel displacement calibration

As mentioned previously, the workpiece holding platform should be designed with enough travel distance in both static and dynamic situation. The static experiment is to test the full-span displacement output of piezoelectric ceramics at rated drive voltage. The dynamic experiment is to determine the working characteristic of the system, because the active vibration cancelation is applied in the micro-grinding in which the main disturbance is likely to occur once per rotation dynamically.

In displacement static output characteristic test, the diving power device is set to manual mode, and the calibration is performed by varying the input voltage from 0 to 120 V in both the ascending and the descending. The calibration result is shown in Fig. 4, the travel distances of the platform is 18 and 15 μm along X- and Y-directions, respectively. It also indicates that the displacement of the platform has a near linear relationship with the change of the voltage. But at the same time, the experiment also shows that the piezoelectric actuator has hysteresis characteristics, which will affect the output of the control displacement, so as to reduce the control efficiency.

The dynamic working characteristic of the piezoelectric ceramic platform is related to the piezoelectric ceramic itself and the power supply performance. In order to test the displacement response ability under the alternating voltage, the piezoelectric ceramic is driven by a sinusoidal voltage, and the displacement of the platform is measured and analyzed. With the driving voltage of 1000 Hz frequency, 24 V amplitude, and

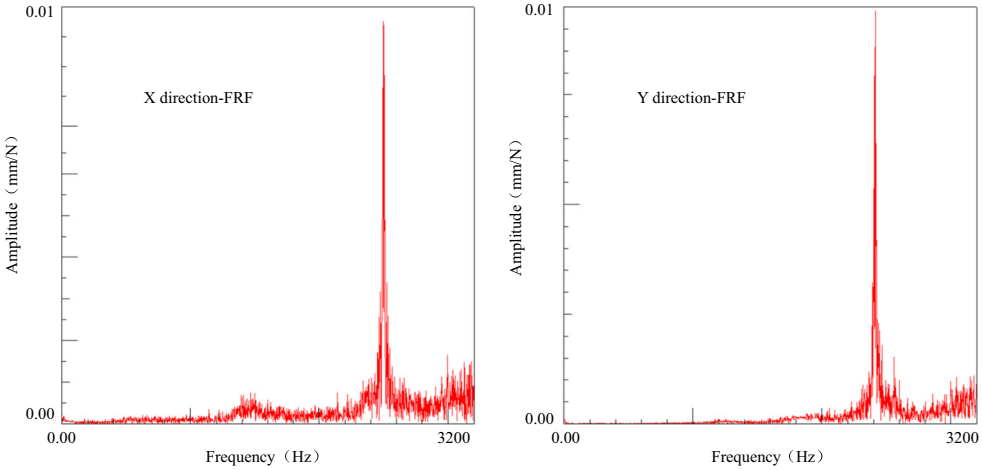

Fig. 3 FRF test of the X/Y-direction

24 V offset, namely $U = 24 + 24\sin(2000\pi t)$, the X, Y-direction displacement response curve is recorded as shown in Fig. 5. In the results, the dynamic displacement amplitude can reach 2.5 and 2.9 μm, respectively under the condition, which could meet the amplitude requirement of active vibration control. Therefore, to combine the nanometer resolution characteristic of piezoelectric ceramic actuator, the system can be effective when the disturbance driving a system to an undesirable response has most of its energy at a high frequency, or perhaps at a fundamental frequency with integer multiples or harmonics of that frequency.

4 System controller design

The Filtered-X Least Mean Square (FXLMS) Algorithm is applied to the controller, which is the active vibration control version of the standard least mean square (LMS) algorithm [25]. The active vibration control can be described as shown in Fig. 6. The control system uses an adaptive filter W(z) to estimate the response of an unknown primary acoustic path P(z) between the reference input sensor and the error sensor. The error signal e(n) is measured by the relative vibration of tool and workpiece. And the signal can be modified by the secondary path function H(z) in the channel from y(n) to e(n). What is more, to account for the effects of the secondary path transfer function H (z), the conventional LMS algorithm needs to be modified. To ensure convergence of the algorithm, the input to the error correlator is filtered by a secondary path estimate C(z).

In the algorithm, the z-transform of error signal e(n) is

$$\mathrm{E(z)} = \mathrm{X(z)} \times \mathrm{P(z)} + \mathrm{X(z)} \times \mathrm{W(z)} \times \mathrm{H(z)} \tag{6}$$

The output y(n) is computed as

$$\mathrm{y(n)} = \sum_{i=1}^{N-1} w_i(n) \times (\mathrm{n-i}) = W^{\mathrm{T}}(n) \times (n) \tag{7}$$

$w_i(n)$ is the 'i'th coefficient of the FIR filter W(z) at time n, and x(n) is the reference signal vector at time n. When this algorithm is implemented, the convergence of the filter can be

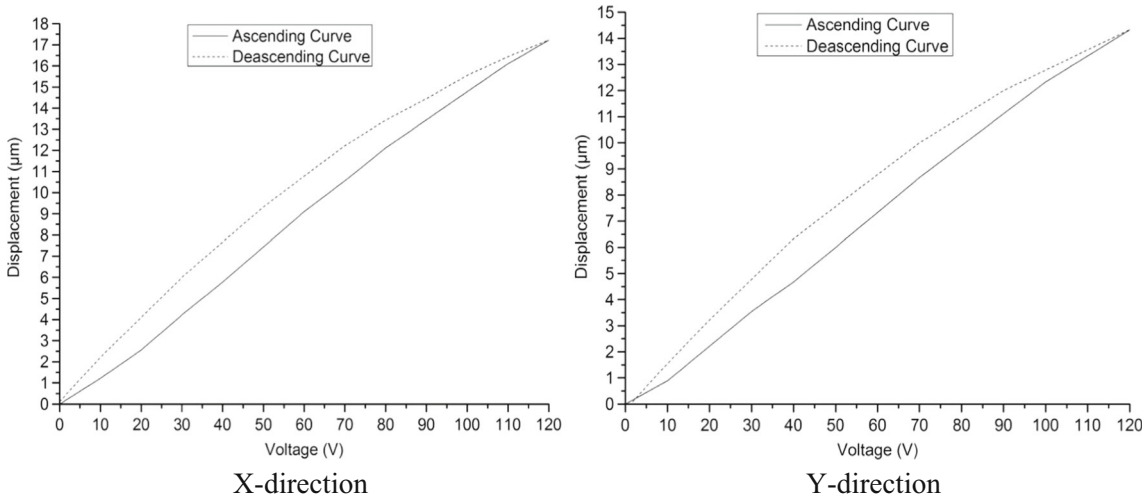

Fig. 4 Displacement characteristic curve of the X/Y-direction

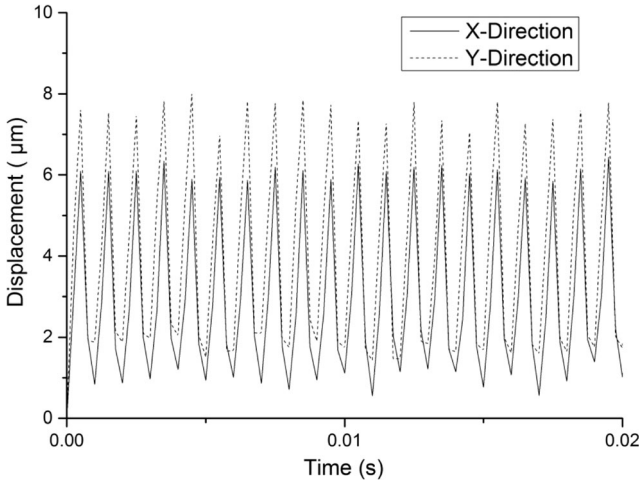

Fig. 5 Dynamic displacement output curve under the driving voltage of $U = 24 + 24\sin(2000\pi t)$

achieved much more quickly than what the theory suggests, and the algorithm appears to be very tolerant of errors made in the estimation of the secondary path H(z) by the filter C(z).

In the controller, the secondary path is a key factor that affects the performance of the control system, for example, the convergence and the effectiveness of the control system. Therefore, in the active control system, the transfer function H(z) should be identified first. In physics, secondary path H(z) includes D/A, power amplifier, active actuator, A/D, and so on. In the paper, assuming the characteristics of H(z) are unknown but time invariant, the off-line testing and modeling technique was used to estimate H(z).

In this approach, the transfer function H(z) can be obtained from its measured frequency response functions via a digital recorder. The measured frequency response functions of the platform along X- and Y-directions are presented in Fig. 7, the characteristics of amplifier, actuator, and the platform are all included in the measured frequency response functions. Then, the nominal parametric can be conveniently derived from the measured results through MATLAB system identification toolbox. The identified parametric transfer function Hx(z) and Hy(z) are given in Eqs. (8) and (9).

$$\mathrm{Hx}(z) = \frac{2.435\times10^{-5}z^4 - 0.5754z^3 + 2.377\times10^{4}z^2 - 4.045\times10^{8}z + 5.285\times10^{12}}{z^4 + 6.923\times10^{3}z^3 + 4.536\times10^{8}z^2 + 1.752\times10^{12}z + 3.69\times10^{16}} \tag{8}$$

$$\mathrm{Hy}(s) = \frac{-5.473\times10^{-8}z^4 - 1.503\times10^{-3}z^3 + 40.23z^2 - 1.651\times10^{6}z + 1.629\times10^{10}}{z^4 + 2.913\times10^{3}z^3 + 2.752\times10^{8}z^2 + 4.191\times10^{11}z + 9.383\times10^{15}} \tag{9}$$

5 Machining verification results and discussions

Typical active vibration cancelation verification is the machining test. The test requires sensors measuring the disturbance unwanted vibration input as well as the actuators' vibration output. To verify the performance of the active vibration control platform in high-frequency micro-grinding, cutting tests are performed. Tool and workpiece vibration signature testing was conducted by a series of engineering experiments to compare the relative vibration amplitude with and without active vibration control.

5.1 Machining experiment

As shown in Fig. 8, the vibration control experiment was performed using a self-developed micro-grinding tool with a Φ1.6-mm metal bonded CBN grinding wheel. The whole assembly of active control platform was fixed onto the Aerotech® XY working stage of the micro-grinding machine. The 20 mm × 10 mm × 2 mm steel workpiece is mounted on the active control platform. The two laser displacement sensors are mounted on the spindle to measure the X/Y vibration displacement of the tool, while the other two laser displacement sensors are mounted on working stage to measure the X/Y vibration displacement of the workpiece or actuator. The

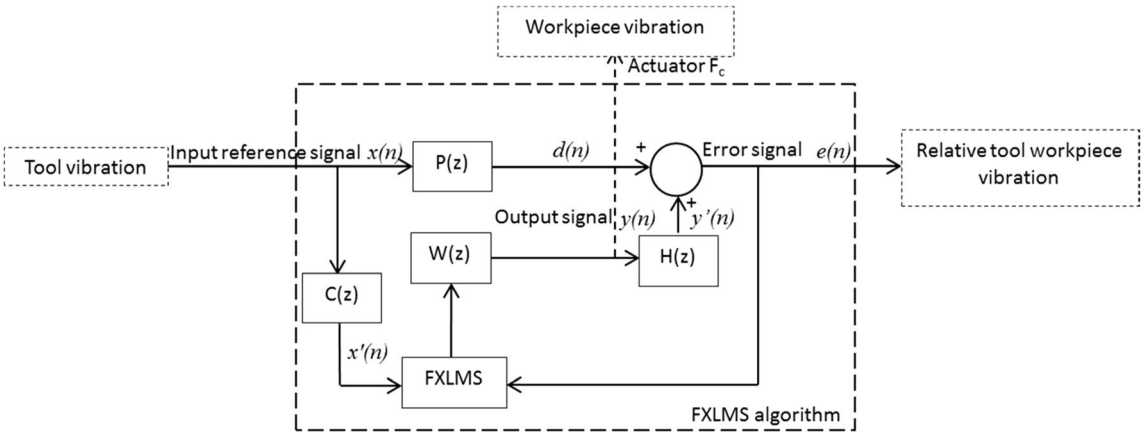

Fig. 6 Block diagram of the FXLMS algorithm control system

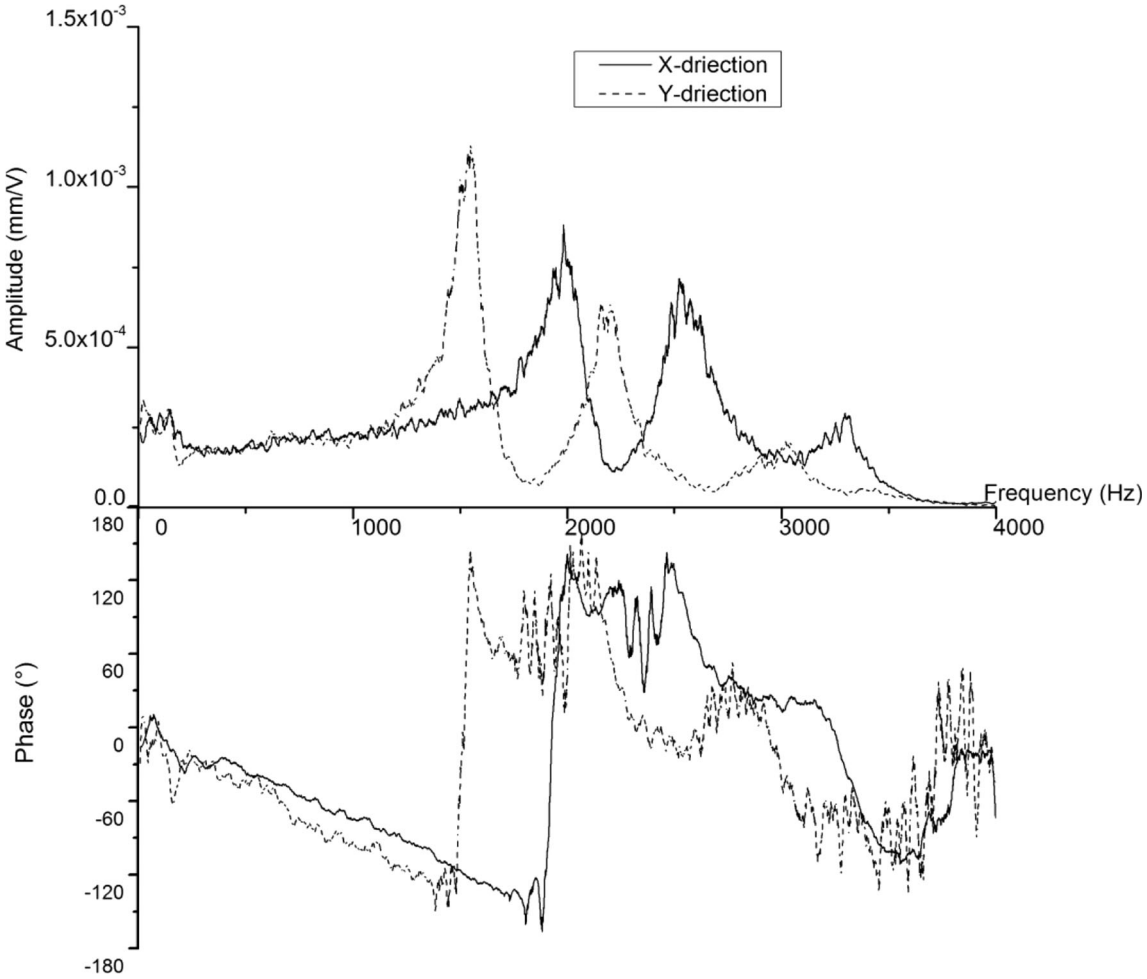

Fig. 7 The frequency response functions curves of the system

roughness of the machined surface is measured by NPFLEX® 3D Surface Metrology System.

The controller designed for active vibration cancelation is implemented by using a personal computer with LabVIEW®,

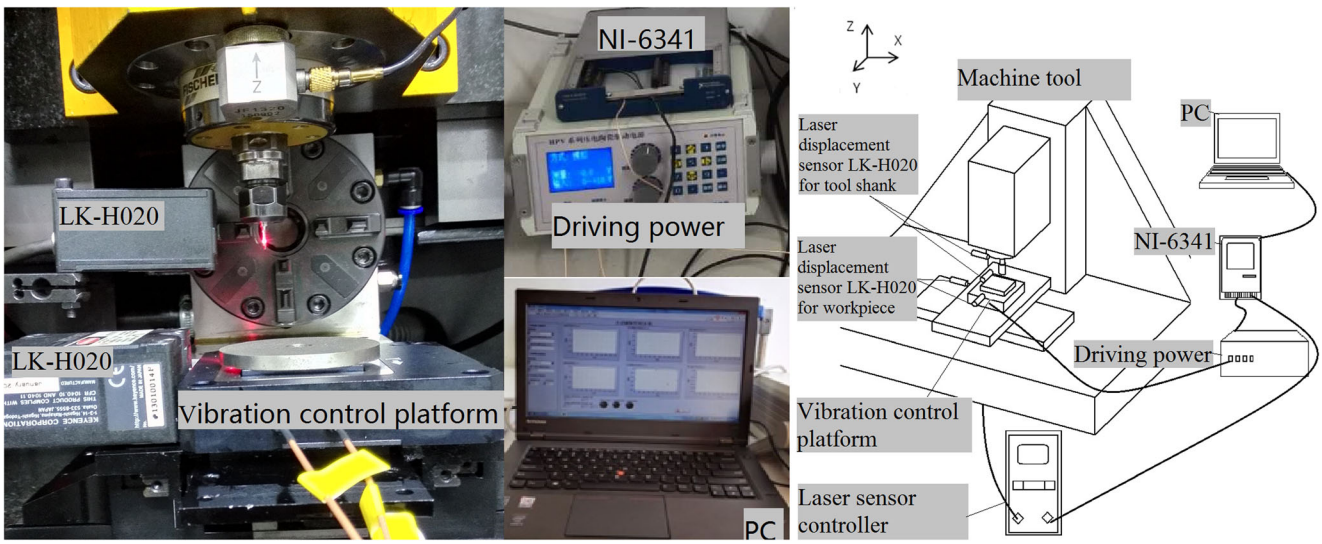

Fig. 8 Machining test experimental setup

Table 1 Machining parameters

No.	Rotating speed (rpm)	Main frequency (Hz)	Feed (mm/s)	Grinding depth (μm)
1	30,000	500	10	5
2	45,000	750	10	5
2	60,000	1000	10	5

and National Instruments® NI-6341 instruments is used as the data acquisition and signal generator [26]. The computational time interval in the control system is 250 us, namely the control frequency is 4000 Hz, which accommodates the vibration frequency to be controlled in the test. In the controller, the relative vibration between the tool and the workpiece is calculated as a feedback signal and control signal is generated to drive the movements of workpiece with the piezoelectric ceramics driving power to cancel the relative vibrations between the tool and the workpiece. Grinding conditions are in Table 1.

5.2 Experimental results and discussions

In this research, the laser vibrometer signal of tool shank contains information on tool vibrations, radial misalignment, and out of roundness; the out-of-roundness of the tool in measurements is negligible. Then the raw signal including and tool vibration and radial misalignment is set as the disturbance x(n) in the test, because they influence the micro-grinding depth in process. And the relative vibration signal namely the displacement signal difference of the tool and the workpiece is the error signal.

To have a sense of the vibration control process, taking the 45,000 rpm (750 Hz) as an example, the measured vibration signal of tool, workpiece, and relative movement is recorded and presented in Fig. 9. It is found that the displacement produced by the active control platform cannot completely cancel the tool vibration because of the time delay. In fact, the time delay phenomenon of vibration control is unavoidable, and there are two main reasons: one is system hardware, including the signal acquisition device and signal output device; the other is the algorithm, including the signal processing and control algorithms such as FXLMS. Thus, the original governing Eq. (10) is converted to (11)

$$M\ddot{x}(t) + C\dot{x}(t) + Kx(t) = F(t) + F_C(t) \tag{10}$$

$$M\ddot{x}(t) + C\dot{x}(t) + Kx(t) = F(t) + F_C(t-\tau) \tag{11}$$

Where τ is the delay value. In this research, the control algorithm does not consider the influence and compensation of time delay and it need further study in the future.

To verify the performance of active vibration control system in micro-grinding, the measured relative vibration between the tool and the workpiece for micro-grinding test with and without control are presented in Fig. 10. By comparing the vibration amplitude in Table 2, one can find the amplitudes of cutting vibrations are attenuated about 30–40%. What is more, the surface roughness results with and without control show that vibration control system improves the surface quality under the machining condition by reducing the tool-workpiece grinding vibration. This indicates that the designed controller works well in cutting vibration cancelation for test.

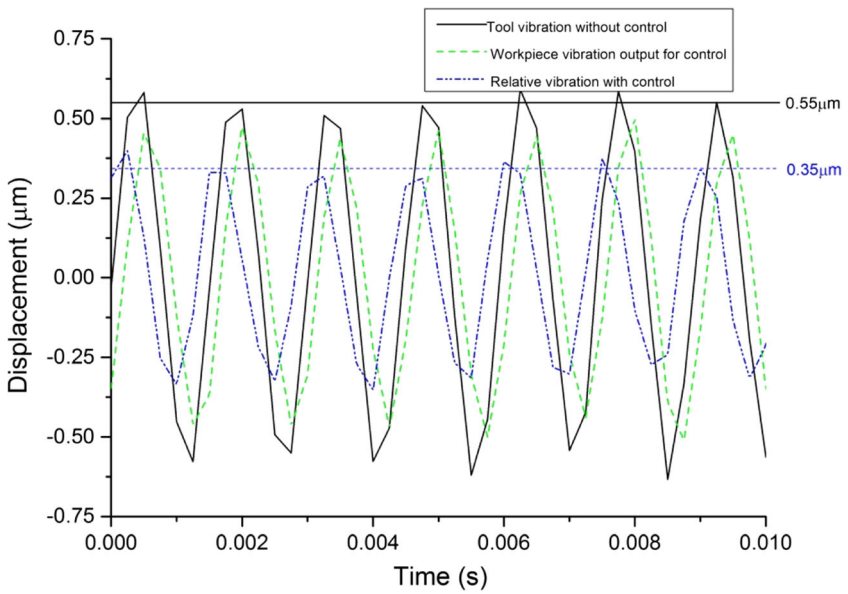

Fig. 9 The vibration control signal in process of 45,000 rpm

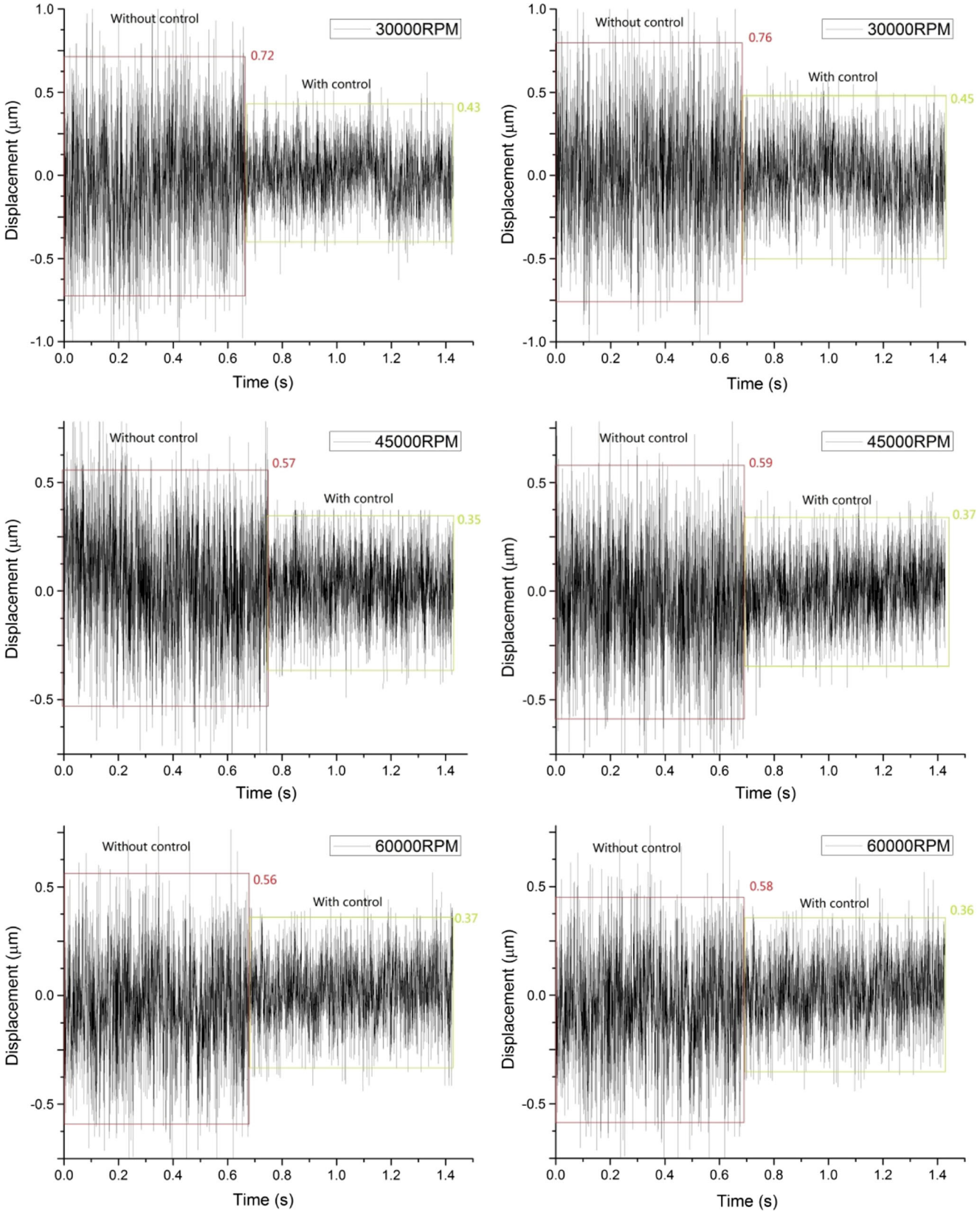

Fig. 10 Comparison of relative vibrations with and without control in micro-grinding

Table 2 Comparison of relative vibration amplitudes with and without control in micro-grinding

Rotating speed (rpm)	Series no.	X-direction vibration amplitude (μm)		Y-direction vibration amplitude (μm)		Average decrease efficiency		Average roughness Ra (μm)	
		Without control	With control	Without control	With control	X	Y	Without control	With control
30,000	1	0.72	0.43	0.76	0.45	39.8%	39.4%	0.85	0.70
	2	0.66	0.40	0.69	0.45				
	3	0.63	0.38	0.66	0.38				
45,000	1	0.57	0.35	0.59	0.37	38.2%	38.2%	0.74	0.63
	2	0.55	0.35	0.58	0.36				
	3	0.63	0.38	0.61	0.37				
60,000	1	0.56	0.37	0.58	0.36	34.9%	34.0%	0.59	0.50
	2	0.58	0.36	0.59	0.38				
	3	0.52	0.35	0.6	0.43				

However, with the increase of the speed, the vibration reduction efficiency decreases while the control frequency increases. These results indicate that the designed active vibration control system can achieve robust disturbance rejection against variations of high-frequency micro-grinding tool vibrations. In this research, as the control system works on the main frequency of the vibration. The bandwidth of the system is based on the main frequency of the vibration; therefore, it will limit the relative vibration decrease efficiency in compensating high-frequency vibrations.

6 Conclusions

In this paper, an active vibration control platform that can be used to suppress the relative vibrations between the tool and the workpiece during the high-speed micro-grinding processes is developed and presented. The platform is applied as a workpiece holding platform and can cancel vibration in real time by sensing the tool vibration with the vibrometer. The specially designed two DOFs vibration control platform with a modal frequency more than 2000 Hz and static travel distance more than 15 μm can cover the vibration cancelation requirement of the micro-grinding process, in which the main vibration frequency can reach up to 1500 Hz, and maximum main vibration amplitude can be 1.5 μm of self-excited and 0.6 μm of forced vibration.

For application of the active vibration control platform, the performance parameters of the control system are obtained through analysis and experiment. The control algorithm of FXLMS is analyzed and computed in the controller, making it conventional approaches to solving vibration problems in the process, in which the tool vibrations in micro-grinding are treated as disturbances to the system; the relative vibrations are tool and workpieces that are set as the control target. Cutting experiments are performed to validate the effectiveness of the control system, and the results show that the developed system works well in high-frequency cutting vibration cancelation.

Acknowledgements This project is supported by the National 863 High Technology R&D Program (no. 2012AA041309) and the Natural Science Foundation of China (no. 50975046).

References

1. Liang SY (2006) Mechanical machining and metrology at micro/nano scale. Proc of SPIE 6280, Third International Symposium on Precision Mechanical Measurements, 628002
2. Aurich JC, Engmann J, Schueler GM, Haberland R (2009) Micro grinding tool for manufacture of complex structures in brittle materials. CIRP Ann Manuf Technol 58(1):311–314
3. Hassui A, Diniz AE (2003) Correlating surface roughness and vibration on plunge cylindrical grinding of steel. Int J Mach Tool Manuf 43(8):855–862
4. Cao Y, Guan J, Li B, Chen X, Yang J, Gan C (2013) Modeling and simulation of grinding surface topography considering wheel vibration. Int J Adv Manuf Technol 66(5–8):937–945
5. Chen J, Fang Q, Li P (2015) Effect of grinding wheel spindle vibration on surface roughness and subsurface damage in brittle material grinding. Int J Mach Tools Manuf 91:12–23
6. Chen S, Cheung C, Zhao C, Zhang F (2017) Simulated and measured surface roughness in high-speed grinding of silicon carbide wafers. Int J Adv Manuf Technol 91(1–4):719–773
7. Wang X, Yu T, Dai Y, Shi Y, Wang W (2016) Kinematics modeling and simulating of grinding surface topography considering machining parameters and vibration characteristics. Int J Adv Manuf Technol 87(9):2459–2470
8. Grigoriev SN, Starkov VK, Gorin NK, Krajnik P, Kopač J (2014) Creep-feed grinding: an overview of kinematics, parameters and effects on process efficiency. Strojniški vestnik J Mech Eng 60(4): 213–220
9. Barrenetxea D, Marquinez JI, Alvarez J, Fernandez R, Gallego I, Madariaga J, Garitaonaindia I (2012) Model-based assistant tool for the setting-up and optimization of centerless grinding process [J]. Mach Sci Technol 16:501–523
10. Pawar PJ, Rao RV, Davim JP (2010) Multiobjective optimization of grinding process parameters using particle swarm optimization algorithm. Mater Manuf Process 25(6):424–431

11. Duncan GS, Tummond MF, Schmitz TL (2005) An investigation of the dynamic absorber effect in high-speed machining. Int J Mach Tools Manuf 45(4–5):497–507
12. Muhammad BB, Wan M, Feng J, Zhang W (2017) Dynamic damping of machining vibration: a review. Int J Adv Manuf Technol 89(9):2935–2952
13. Ganguli A, Deraemaeker A, Preumont A (2007) Regenerative chatter reduction by active damping control. J Sound Vib 300: 847–862
14. Tewani SG, Rouch KE, Walcott BL (1995) A study of cutting process stability of a boring bar with active dynamic absorber. Int J Mach Tools Manuf 35(1):91–108
15. Zhang YM, Sims ND (2005) Milling workpiece chatter avoidance using piezoelectric active damping: a feasibility study. Smart Mater Struct 14:65–70
16. Chen F, Liu G (2017) Active damping of machine tool vibrations and cutting force measurement with a magnetic actuator. Int J Adv Manuf Technol 89:691–700
17. El-Sinawi AH, Kashani R (2005) Improving surface roughness in turning using optimal control of tool's radial position. J Mater Process Technol 167:54–61
18. Al-Zaharnah IT (2006) Suppression vibration of machining processes in both feed and radial directions using optimal control strategy: the case of interrupted cutting. J Mater Process Technol 172:305–310
19. Zhang X, Shinshi T, Li L, Shimokohbe A (2003) A combined repetitive control for precision rotation of magnetic bearing. Precis Eng 27:273–282
20. Rashid A, Nicolescu CM (2006) Active vibration control in palletised workholding system for milling. Int J Mach Tools Manuf 46:1626–1636
21. Brecher C, Manoharan D, Ladra U, Köpken HG (2010) Chatter suppression with an active workpiece holder. Prod Eng 4:239–245
22. Long X, Jiang H, Meng G (2013) Active vibration control for peripheral milling processes. J Mater Process Technol 213(5):660–670
23. Guo M, Li B, Yang J, Liang SY (2016) Influence of dynamic force on vibration of micro-machine tool spindle. Proceedings of the International Conference on Advanced Materials, Structures and Mechanical Engineering, 217–222
24. Test LMS (2009) Lab User manual. LMS INTERNATIONAL, Leuven
25. Kuo SM, Morgan DR (1999) Active noise control: a tutorial review. Proc IEEE 87(6):943–973
26. Ponce-Cruz P, Ramrez-Figueroa FD (2010) Intelligent Control Systems with LabVIEW. Springer, London